Journal of Molecular Catalysis A: Chemical 335 (2011) 136–144

Contents lists available at ScienceDirect

Journal of Molecular Catalysis A: Chemical

journal homepage: www.elsevier.com/locate/molcata

Preparation and characterization of TiO_2/carbon composite thin films with enhanced photocatalytic activity

Raja Sellappan[a,*], Jiefang Zhu[b], Hans Fredriksson[a], Rafael S. Martins[a], Michael Zäch[a], Dinko Chakarov[a]

[a] Department of Applied Physics, Chalmers University of Technology, 41296 Gothenburg, Sweden
[b] Department of Materials Chemistry, Uppsala University, SE-751 21 Uppsala, Sweden

ARTICLE INFO

Article history:
Received 20 August 2010
Received in revised form
21 November 2010
Accepted 23 November 2010
Available online 2 December 2010

Keywords:
Titanium dioxide
Carbon
Thin film
Characterization
Photocatalysis
Methanol decomposition

ABSTRACT

Composite TiO_2/carbon thin films prepared by physical vapor deposition techniques on fused silica substrates show enhanced photocatalytic activity towards decomposition of methanol to CO_2 and water, as compared to pure TiO_2 films of similar thickness. Raman and XRD measurements confirm that annealed TiO_2 films exhibit anatase structure while the carbon layer becomes graphitic. Characteristic for the composite films is an enhanced optical absorption in the visible range. The presence of the carbon film causes a shift of the TiO_2 absorption edge and modifies its grain size to be smaller. We hypothesize that the observed enhancement of photocatalytic activity is due to synergy effects at the carbon/TiO_2 interface, resulting in smaller titania crystallite size and anisotropic charge carrier transport, which in turn reduces their recombination probability.

1. Introduction

Titanium dioxide is a well-known and widely studied photocatalyst especially after the pioneering work of Fujishima and Honda on water splitting with light [1]. Ever since it has been of great interest due to potential applications for environmental remedies such as purifying organic waste or cleaning air pollutants [2], for energy conversion technologies such as in solar cells [3], production of "solar" hydrogen [1], etc. TiO_2 is recognized for its characteristic properties such as strong oxidation potential of photogenerated holes, chemical stability, non-toxicity and low cost. TiO_2 crystallizes in three crystal phases; anatase, rutile and brookite, among which the anatase phase typically has a higher photocatalytic activity due to its band position with respect to the hydrogen redox potential [4]. However, it has some practical limitations in absorbing the visible part of the electromagnetic spectrum due to its wide bandgap (~3.2 eV), and it suffers from fast electron-hole recombination [5]. Since the ultraviolet (UV) portion of solar radiation at the earth surface constitutes only 5% of the total, it is highly desirable to extend the light absorption of the photocatalyst in the visible range.

Among the many attempts in this direction, modification with carbon (C) has been an efficient route to alter the photocatalytic properties of TiO_2 [6–8]. Carbon itself plays an important role in a number of heterogeneous catalytic processes acting as adsorbent, catalyst support or active material [9]. In particular, the properties of graphitic carbon films, such as good conductivity and high light absorption in the visible range, are utilized for photocatalytic applications [9].

Carbon as a dopant in TiO_2 improves the optical absorbance in the visible spectral range by introducing localized energy states in the bandgap, but at the same time increases the electron-hole recombination probability [10]. Doping and addition of carbon to TiO_2 catalysts, where the carbon atoms substitute oxygen or titanium atoms or occupy interstitial sites, can be achieved in different ways, and there are several reports on the positive catalytic effect of these procedures [8,11,12]. Despite these observations, it is critically argued that experimental evidence for the enhancement of photocatalytic reactions with visible light for the carbon-doped system is still missing or at least controversial [13]. Several studies also suggest that TiO_2 on an activated carbon matrix simply enhances the surface area and hence more reactants can adsorb on the surface of the catalyst for photocatalytic degradation of pollutants [14,15]. Similarly, recent work describing how carbon nanotubes have been employed as a support for TiO_2 is assigned to improvements of the photo-response due to improved conductivity and dispersion of the system [7,16–18]. With these previous results as a reference, we

* Corresponding author at: Fysikgrand 3, F5121, Chalmers University of Technology, 41296 Gothenburg, Sweden. Tel.: +46 31 7723373; fax: +46 31 772 31 34.
E-mail address: rayas@chalmers.se (R. Sellappan).

1381-1169/$ – see front matter © 2010 Elsevier B.V. All rights reserved.
doi:10.1016/j.molcata.2010.11.025

have chosen to introduce carbon as a separate film and investigate its role in a well-defined and simple model system of C/TiO_2 thin composite film. The main investigated parameters are the thickness of the films and the effect of annealing on the morphology and optical properties of TiO_2.

Takahashi et al. [5] have suggested that the efficiency of TiO_2 is decreased due to recombination of the photo-generated carriers at trapping sites both in the bulk and at the surface. Therefore, films with smaller thickness are expected to show reduced (bulk) electron-hole recombination. This is the reason to restrict the thickness of investigated films to no more than 100 nm. It is also expected that interface effects will play an important role, which could be sensed at a certain TiO_2 thickness; meaning for thick TiO_2 films, the underlying carbon film will no longer play a role. Li and Gray [19] have suggested that the interface between solid particles of the same kind or different kinds act as a 'hot-spot' for enhanced photocatalytic activity. Another issue of interest is related to synergy effects at the interface between the films and how they affect the charge transport as well as the photocatalytic activity.

While the primary aim of this work is to understand how a thin, graphitic-like carbon film enhances the optical absorption in the visible range, and what are the structural changes of TiO_2 deposited on carbon, another aim of the study is to provide a base for comparison with core-shell and other self assembled TiO_2/C composites [10,20]. Hitherto, little work has been carried out on graphitic-like carbon material with TiO_2 for photocatalytic and photoelectrochemical applications [10,21,22]. We hope that this work will lead to further improvements in this direction.

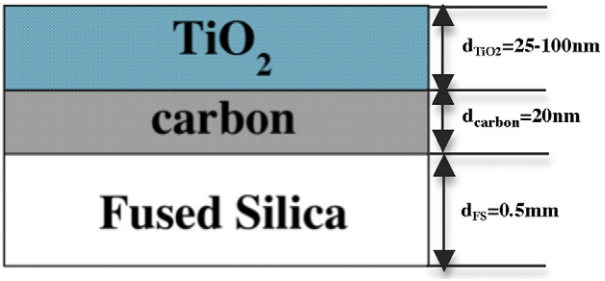

Fig. 1. Schematic structure of the prepared samples with respective thickness of the carbon and titania films.

2. Experimental

2.1. Sample preparation

Fig. 1 shows the schematic structure of the investigated samples. The first fabrication step was the deposition of a carbon film on a fused silica substrate (Double side polished (DSP), University wafer). This was followed by TiO_2 deposition onto the carbon film. Before deposition, the substrates were cleaned by a standard procedure that includes washing in acetone and iso-

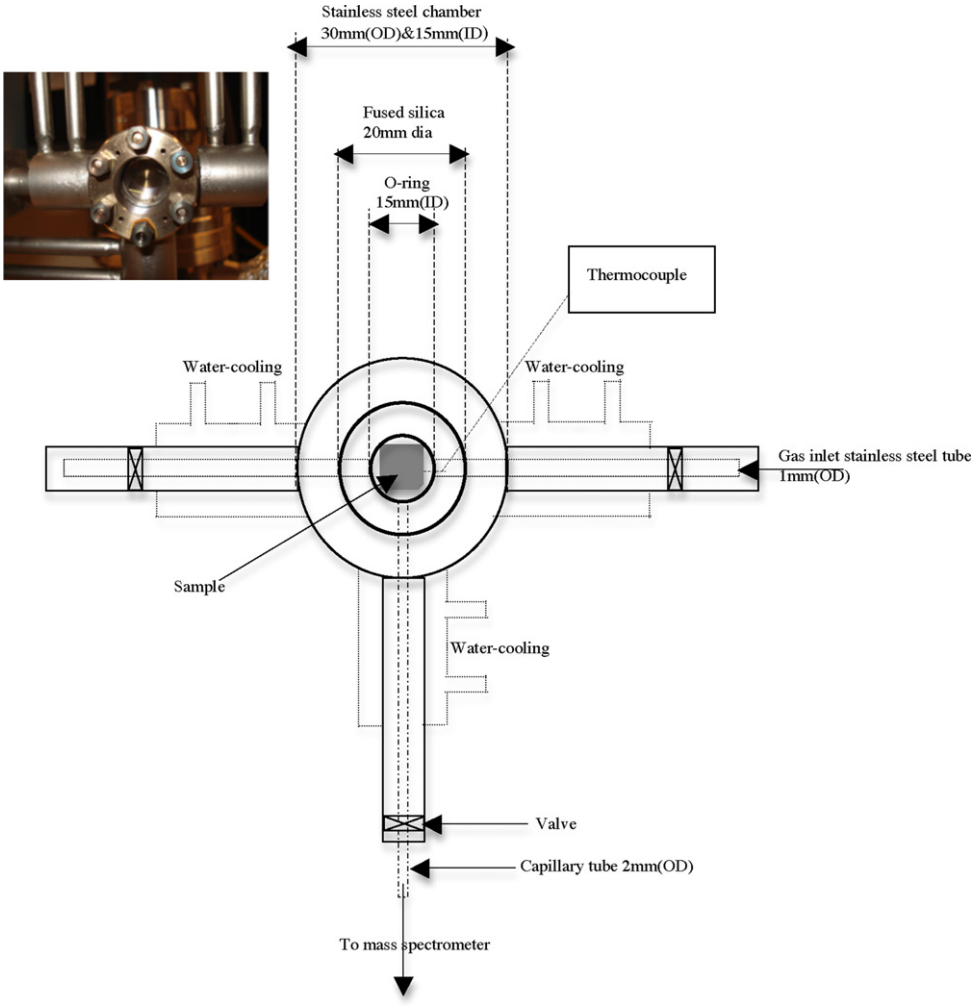

Fig. 2. Schematic of the photocatalytic microreactor setup used in this work; the inset shows a photograph of the reactor chamber.

Table 1
Sample types with their respective thickness and description of different characterization performed on samples.

Sample type	Thickness in nanometer (nm)	Thermal annealing	Characterization
FS/C	20	Yes and no	AFM, XRD, Raman, optical, PCM
FS/TiO_2	35[a]	Yes and no	AFM, XRD, Raman, optical, PCM
FS/TiO_2	50[a], 65[a], ~100[a]	Yes	AFM, optical, PCM
FS/C/TiO_2	20 + 35	Yes and no	AFM, XRD, Raman, optical, PCM
FS/C/TiO_2	20 + 35	Yes: Carbon No: TiO_2	Optical
FS/C/TiO_2	20 + 25	Yes	Optical
FS/C/TiO_2	20 + 50	Yes	AFM, XRD, Raman, optical, PCM
FS/C/TiO_2	20 + 65	Yes	AFM, XRD, Raman, optical, PCM
FS/C/TiO_2	20 + ~100	Yes	AFM, XRD, Raman, optical, PCM

FS, fused silica substrate; AFM, atomic force microscopy; XRD, X-ray diffraction; PCM, photocatalytic measurement; no, as-deposited film.
[a] The estimated variation of TiO_2 thickness = (±~3–5%).

propyl alcohol in an ultrasonic bath and oxygen plasma etching (Plasma Therm Batchtop RIE 95(m)). The size of the samples, as determined by the requirements for the photocatalytic and optical measurements, was 1 cm × 1 cm and 1.7 cm × 1.7 cm, respectively.

The carbon film was deposited in an electron beam evaporation system (AVAC HVC-600, at a base pressure between 3 and 7×10^{-6} mbar) using graphite as a source material. The deposition was performed after degassing the source for a few minutes and establishing a constant evaporation rate (monitored by a Quartz Crystal thin film monitor). Carbon film of desired thickness (20 nm) was deposited at a deposition rate of ~1 Å/s.

TiO_2 was deposited by DC reactive magnetron sputtering (FHR MS150). The base pressure of the chamber was maintained at high vacuum (10^{-7} mbar range), and the working pressure was kept at about 5×10^{-3} mbar. The resulting film thickness was measured after the deposition with the help of a surface ellipsometer (J.A. Woollam M2000).

Post-deposition annealing was carried out with the help of a rapid thermal processing (RTP) system (JIPELEC Jet First 200) for 5 min in Argon atmosphere. The cooling time was set to 5 min.

A number of samples were prepared by the methods described above and their parameters are summarized in Table 1.

2.2. Sample characterization

The samples were characterized with a variety of techniques with focus on their optical and morphological properties. The surface morphology of the samples was characterized with an AFM (DI Dimension 3000 SPM) operated in tapping mode and using silicon tips with a tip radius below 5 nm. The structural characterization was done by XRD and Raman spectroscopy. The XRD characterization was carried out with a help of a Siemens D5000 diffractometer with a step size of 0.03 deg and time/step of 2 s. The Raman measurements were carried out by a LabRam Raman spectrometer using a He–Ne laser of 632.8 nm light with a beam intensity of 1.76 mW. Optical measurements were carried out with the help of a Cary Varian-500 double-beam spectrophotometer and a diffuse reflectance accessory (DRA).

2.3. Photocatalytic experiments

The photocatalytic tests were performed in a home-built stainless steel microreactor (reactor volume 880 μl) coupled with an on-line mass spectrometer (VG instruments SX200 quadrupole mass analyzer) for detection and analysis of the reaction products. The overall reactor and the irradiation setup are shown in Fig. 2. The cylindrical reactor chamber is closed on both sides with optically flat fused silica windows (Oriel, 20 mm diameter, 1 mm thickness) and sealed with Viton© O-rings and standard 30 mm (outer) diameter stainless steel miniflanges (KJLesker). The sample (and reactor)

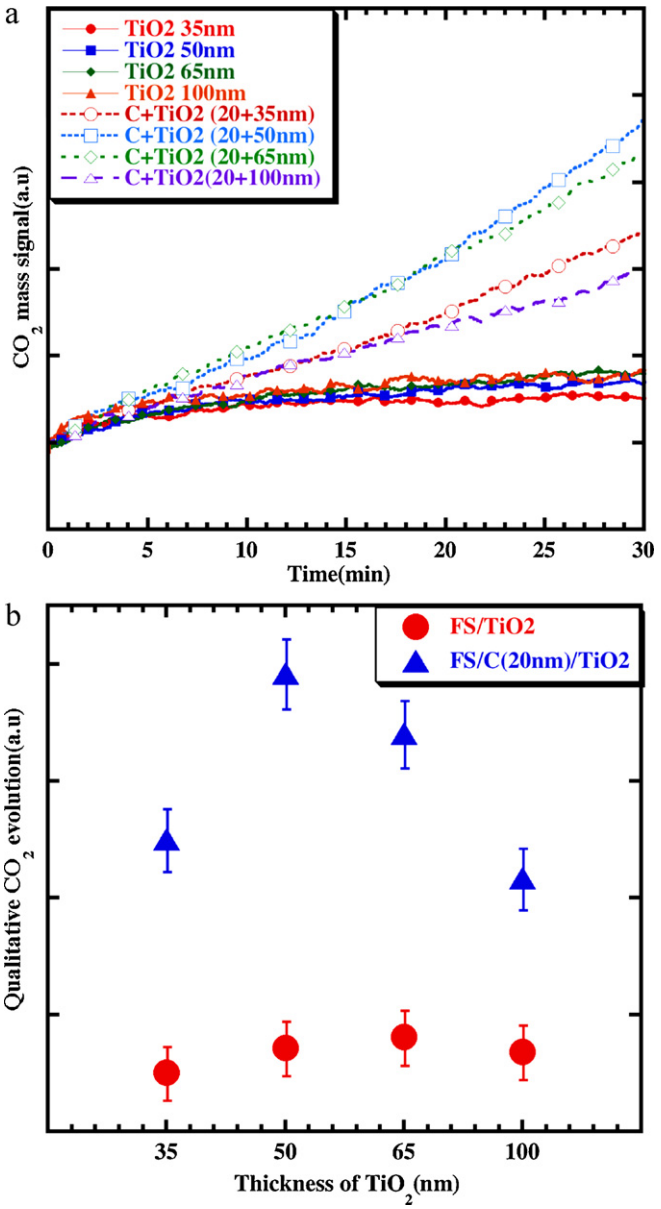

Fig. 3. (a) CO_2 mass spectrometer signal ($m/z = 44$) from methanol photodecomposition on TiO_2/C samples with different thicknesses. The signals are normalized to the background CO_2 concentration. The UV light illumination is turned on at $t = 0$. (b) Qualitative plot of CO_2 evolution for films of different thicknesses. The plot was obtained by integrating the data shown in (a).

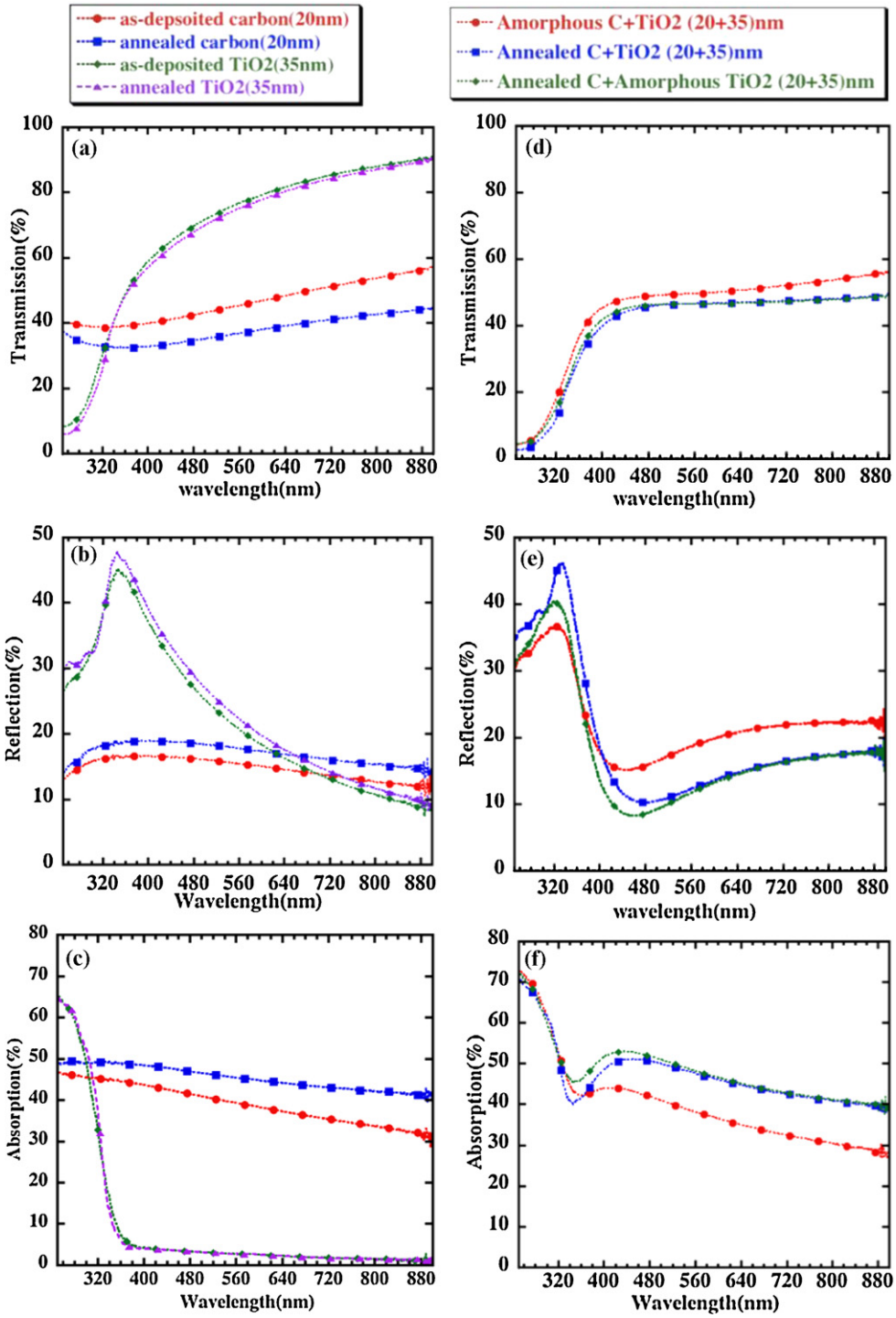

Fig. 4. Optical measurements of individual and composite films of C (20 nm) and TiO_2 (35 nm) on fused silica: (a) transmission, (b) reflection, (c) absorption, (d) composite films transmission, (e) composite films reflection and (f) composite films absorption.

temperature was controlled by external heating of the reaction cell and water-cooling. The temperature was measured directly by a thermocouple placed inside the reactor and in contact with the sample. The average reactor temperature during the experiments described here was about 16 °C. The light induced heating under irradiation of the sample was maximum 5 °C. The pressure in the reactor chamber was measured with a capacitance manometer and could be varied between 5×10^{-3} and 1000 mbar. The gases from the reactor were let into the mass spectrometer (MS) chamber via a capillary leak. The reactor volume was filled with a mixture of methanol (10 μl) and oxygen gases from a small stainless steel container. The monitored products of methanol photo-oxidation were carbon dioxide and water (m/z = 44 and 18, respectively). The measurements were performed in batch mode.

The non-polarized photon source used in the measurements was a continuous wave (cw) system (PTI) based on a 75/100 W Xe/Hg arc lamps with a combination of focusing lenses, apertures, neutral density filters and bandpass filters. The system allows accu-

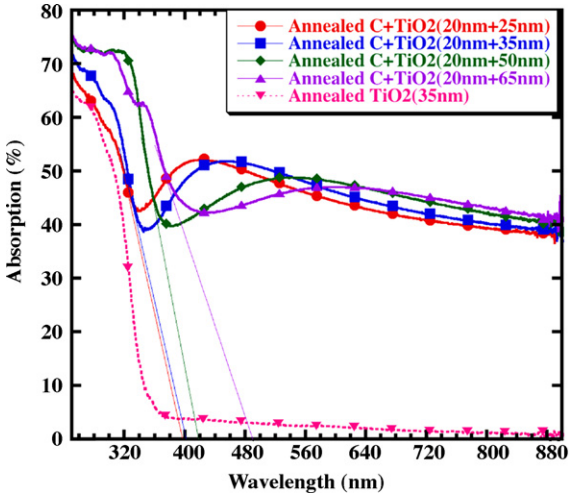

Fig. 5. Optical absorption of composite films with different thicknesses of TiO_2 deposited on fused silica. Absorption edge has been marked by a tangent line for all spectra.

rate control of the photon wavelength and flux on the sample. In particular, a short pass filter (Thermo Oriel) with 85% transmission between 250 nm and 400 nm was used. The irradiation was made through the UV transparent (Fused silica) and O-ring sealed reactor window (see Fig. 2). The backside window (of the same type) provides possibility for direct optical measurements of the transmitted light through the sample. The output power from the optical system was measured in air by focusing the light onto a thermopile power sensor mounted in an Isoperibol enclosure (Scientech). Focusing lens, apertures and the use of neutral density filters could regulate the photon flux on the sample surface. The typical light intensity used in the measurements was 120 mW/cm^2.

The measurements were performed according to the following procedure: the reactor containing the sample was annealed and evacuated. After cooling it down to 16 °C, the reactants were let into the reactor, and the valve to the mass spectrophotometer was opened. Once the reactants pressure has reached equilibrium, the MS background signals were recorded. Then the sample was irradiated, while continuously monitoring the reactor pressure, temperature and gas composition.

3. Results and discussions

The methodology of this study was to systematically analyze the effects of the different preparation steps, such as deposition order and annealing conditions, on the optical and morphological characteristics of the samples. These observations were then correlated with changes in measured photocatalytic performance. Another parameter in the study was the TiO_2 film thickness, which we varied between 25 nm and 100 nm.

Both the carbon and TiO_2 films are amorphous after deposition. The e-beam evaporated carbon film, using graphite as a source material, is mostly amorphous, but annealing above 700 °C makes it graphitic and conducting [23,24].

TiO_2 was deposited onto the annealed carbon film and then the samples were annealed at the same condition as carbon at 500 °C. It is known that annealing TiO_2 in the range between 400 and 600 °C will make it crystallize in the anatase phase [25], which in turn has a higher photocatalytic activity [26]. The reason for using rapid thermal processing (RTP) in argon atmosphere was to prevent carbon oxidation.

3.1. Photocatalytic measurements

The test reaction for evaluation of the photocatalytic activity of fabricated samples was oxidation of gas phase methanol (CH_3OH) to CO_2 and H_2O (Eq. (1)). These measurements are indicative for the overall activity of the films and are also able to discriminate the effect of thickness and the optical absorption on charge transport and separation of the generated charge carriers. Typical MS traces for the films are shown in Fig. 3(a).

$$2CH_3OH + 3O_2 \rightarrow 2CO_2 + 4H_2O \quad (1)$$

TiO_2 films of different thickness showed significantly different activity. As the film thickness increases up to 65 nm, the CO_2 evolution also increases and then starts to decrease or saturate around 100 nm. We suggest that once the film thickness reaches beyond the charge carrier mean free path, the film thickness will cease to play a role for the reaction rate. On the other hand, the large volume of the thicker film will increase the total absorption of the system.

TiO_2 films deposited on carbon showed higher photocatalytic activity compared to the same TiO_2 films deposited directly on fused silica. Similarly to the pure TiO_2 films, the activity increases up to a certain thickness (~50 nm in this case) and then decreases for thickness larger than ~65 nm. This trend is illustrated qualitatively in Fig. 3(b). From these measurements it is possible to distinguish the effect of TiO_2 film thickness on the photocatalytic activity for samples with and without a carbon film underneath.

Based on our observations and comparing with similar studies [10,16], we hypothesize that possible reason for the observed increase in photocatalytic activity of the composite films are effects at the interface of TiO_2 crystallites and the carbon films that contribute to efficient separation of the generated charge carriers. The hole would move to the surface of the TiO_2 film, and the electron would be conducted away from the interface and transferred to the carbon film. On the other hand, the charge transport will be restricted within the mean free path (e_τ) and thus thicker films above e_τ will not show an increased activity.

In order to prove that the observed variations of CO_2 signal are due to methanol oxidation but not to oxidation of the carbon film, we performed control measurements on a bare carbon film with methanol and composite films without methanol under UV illumination. The result undoubtedly showed no CO_2 evolution in both cases. Strong UV irradiation of the reactor interior, even without any sample always produces slight increase of all background signals, including CO_2. However, based on such control measurements we can with confidence trace the origin of the increase. We note that as-deposited films did not show any activity in this work, and no activity was observed in dark. It may be expected that upon annealing of composite films, the carbon may react with oxygen atoms in the titania lattice and produce oxygen vacancies in the film [27]. However, considering the sequential deposition and annealing (Note that carbon film becomes graphitic before deposition of TiO_2.), we assume that the carbon-related variation of the amount of oxygen vacancies and their respective contribution to the activity is negligible.

From the photocatalytic measurement, we suggest that the carbon film plays a role in increasing the relaxation time [28] of the generated charge carriers in the TiO_2 film. It is possible to find an optimum thickness of the photocatalyst to increase the quantum efficiency. We suggest, however, that the optimum thickness depends on the quality of the film, including its crystallinity and the number of localized sites or traps etc.

We further believe that the photocatalytic activity has a strong dependence on the optical absorption, surface area and crystalline phase of the films since they are the main governing parameters in the photocatalytic reaction. We try to correlate these parameters with the observed increase in photo-activity in the next sections.

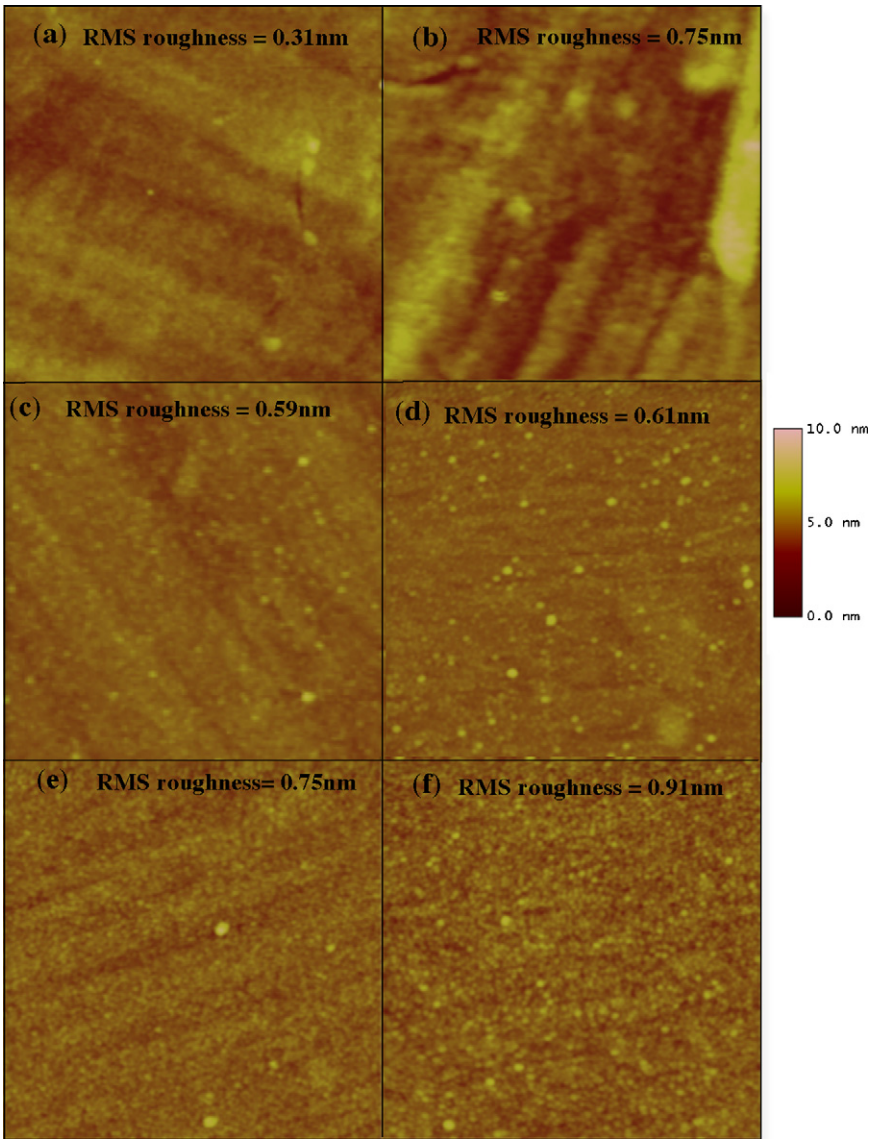

Fig. 6. AFM images of amorphous and annealed carbon films (a and b, respectively); amorphous and annealed TiO_2 films (c and d, respectively); amorphous and annealed $C+TiO_2$ composite films (e and f, respectively). Fused silica was used as a substrate, and the scan size was 1 μm × 1 μm. The RMS roughness is mentioned on each image.

3.2. Optical characterization

The optical absorption (A) of the sample is determined as:

$$A(\%) = [1 - (T + R)] \times 100 \quad (2)$$

where T and R are the measured transmission and reflection in %, respectively.

The optical measurements were performed in two steps; the transmission measurement was done by placing the sample surface perpendicular to the light beam and collecting the transmitted light by placing the detector far behind the sample. The reflectivity measurement was done using an integrating sphere. In this case the active layer of the sample faced the light source, and all backward scattered light was collected in the sphere.

Fig. 4(a)–(f) summarizes the optical measurements of the fabricated samples. The optical absorption of carbon and TiO_2 films, both as-deposited and annealed, is shown in Fig. 4(c). The absorption edge of annealed TiO_2 films appears between 370 and 380 nm, which is in agreement with the width of the bandgap of the anatase, E_g~3.3 eV. One can also note that the absorption edge of amor-

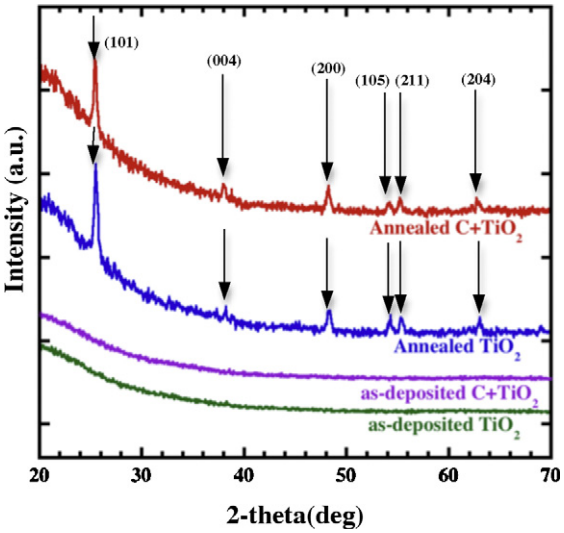

Fig. 7. XRD spectra of as-deposited and annealed TiO_2 with and without carbon on fused silica.

phous TiO_2 is slightly smeared out in comparison with the sharper absorption edge of the annealed films. The measured relatively weak absorption in the visible might be due to reduced TiO_2 [29,30].

The reflectivity of carbon films is below 20% in the visible part of the spectrum followed by a sharp drop in the UV range (see Fig. 4(b)). The result is in accordance with our previous measurements of nanostructured carbon films [31] and confirms the graphitic nature of the film. The annealed carbon film is more reflective, because of its better-ordered structure.

The optical absorption of composite TiO_2/carbon films was calculated from the separate measurements of transmission and reflection (see Fig. 4(d) and (e), respectively)). The optical absorption of these films shows some peculiar features as, for example, an increased absorption around 440 nm (Fig. 4(f)). Comparing and calculating the optical response of films with different thicknesses reveal the origin of this increase. From the analysis of TiO_2 films with different thicknesses deposited on the carbon film (20 nm thick), we conclude that the increase in absorption is due to interferential effects. From the same measurements (see Fig. 5) it is evident that the underlying carbon film causes a red shift of the absorption threshold of TiO_2. The absorption threshold was estimated according to the procedure adopted in [32] and is displayed in Table 2.

Table 2
Absorption threshold of different thicknesses of TiO_2 on carbon films.

Film thickness (nm)	Absorption threshold (nm)
TiO_2 (35)	~375
C + TiO_2 (20 + 25)	396.3
C + TiO_2 (20 + 35)	401.5
C + TiO_2 (20 + 50)	417.9
C + TiO_2 (20 + 65)	495.6

The main observation from our optical measurements is that the composite films absorb strongly in the visible region and exhibit a red-shifted absorption edge in comparison with pure TiO_2 films. Both the shift and the total absorption are more pronounced for thicker TiO_2 films. This is in agreement with the observed trend of the photocatalytic activity with increased film thickness. The effect

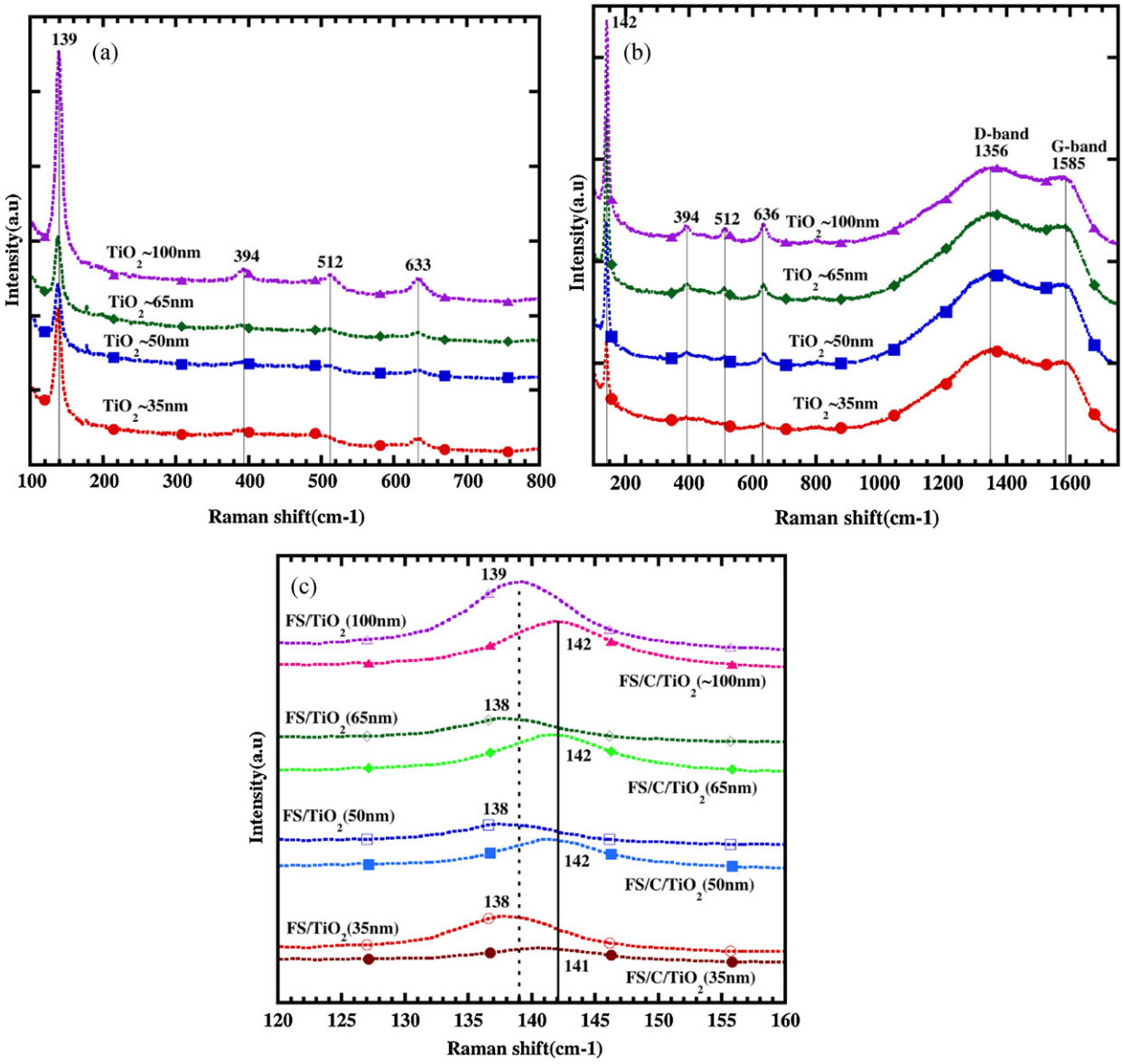

Fig. 8. (a) Raman spectra of TiO_2 films (annealed) with different thicknesses. (b) Raman spectra of composite films (annealed C + TiO_2) with different thicknesses. (c) Raman E_g peak comparison for TiO_2 films (annealed) with and without carbon. The substrate was fused silica (FS) in all cases.

Table 3
FWHM value for the film with different thicknesses of pure TiO_2 and composite films on fused silica.

Film thickness of TiO_2/(C + TiO_2) on fused silica in (nm)	FWHM of E_g peak at 139/(142) (cm^{-1})
35/(20 + 35)	9.6/10
50/(20 + 50)	9.3/9.5
65/(20 + 65)	9.2/10
100/(20 + 100)	9.7/10.2

of thickness is obviously restricted by the mean free path of the charge carriers and above that range, there is only increase of the optical absorption but not of the catalytic activity, see Fig. 3(b).

3.3. Morphology and structural characterization

Fig. 6 shows representative AFM images of the different types of fabricated samples. The morphology of TiO_2 films changes significantly after annealing. This is valid for films deposited both on bare fused silica substrate and the substrate pre-covered with carbon. It is known that the structure of a thin film depends on the substrate or layer on which it is grown [33]. In our case, it is expected that the underlying carbon film will affect the size of the TiO_2 grains. This is indeed manifested by the increased roughness of the composite films. This change in morphology of the composite films may influence the photo-reaction as Li and Gray [19] reported. In this paper, the authors hypothesized that the 'solid–solid interface is a key structural feature that facilitates charge separation to hinder recombination and enhance photocatalytic efficiency'.

From the XRD results shown in Fig. 7, it is clear that the as-deposited TiO_2 films are purely amorphous. Annealing them at 500 °C (with and without carbon underneath) transforms them into the anatase phase. We conclude that the TiO_2 film is polycrystalline with a strong diffraction peak for the ⟨1 0 1⟩-crystal facet. The grain size has been approximately estimated, using the high intensity crystal facet ⟨1 0 1⟩ peak, according to the Scherrer equation by taking background and instrument broadening effects into account. The calculated grain size of the composite films is roughly 16% smaller than for pure TiO_2 films. This result indicates that the grain size of the TiO_2 becomes smaller on the carbon film. This change in crystallite size was manifested in morphology as seen in the AFM study. The noise in the beginning of the XRD scan was attributed to reflection from the substrate.

The Raman spectra of TiO_2 films with different thicknesses grown on fused silica are shown in Fig. 8(a). The result shows that the annealed TiO_2 films are composed of only the anatase phase which is characterized by the Raman peaks (in cm^{-1}) at 139 (E_g mode), 394 (B_{1g} mode), 512 (A_{1g} or B_{1g} mode), and 633 (E_g mode) [34]. As the thickness of the TiO_2 film is increased, the peak intensity of *Eg* also increases which could be related to changes in the optical properties of the material, since the scattering cross section is dependent on the material's optical constants [35,36], and/or enhanced crystallinity in the films [10]. The composite films also exhibit the same anatase phase (see Fig. 8(b)), but there is a peak shift for the E_g modes to higher wave numbers (139 → 142, 633 → 636). The peak shift E_g at 139 cm^{-1}, shown in Fig. 8(c), is correlated to the size of the TiO_2 grains. The full width at half-maximum (FWHM) of the E_g peak at 139 cm^{-1} (142 cm^{-1} for composite films) is displayed in Table 3. There is a small peak broadening effect for the composite films compared to pure TiO_2 films. Several reports correlate this shift, the broadening of peak width and the decrease in intensity to the smaller crystallite size of TiO_2 [37–39]. There is a small variation of all peaks from the reference value [34], which could be attributed to instrumentation (calibration) error.

It is clear from the Raman measurement that the annealed carbon film becomes graphitic (see Fig. 8(b)). The graphitic nature is characterized by the G-band which refers to single crystalline graphitic that has a peak position around 1585 cm^{-1}, and the D-band (∼1356 cm^{-1}) which refers to the intra-band disorder in the hexagonal ring structure in the film [40]. The relative peak intensity (I_D/I_G) of the D- and G-bands is a measure of the degree of graphitization in the film. In contrast, the Raman spectra of as-deposited carbon films show overlapping D and G peaks (not shown). This is interpreted as indicative for the amorphous character of the as-deposited films.

The main finding from the Raman measurements is that the TiO_2 grains become smaller in the composite films than in pure TiO_2 films. The smaller grain size of TiO_2 could be one of the possible reasons for the enhanced activity of the composite films due to an increase in surface area, in addition to the synergy effect. We note that the crystallite size is not related to the film thickness. On the other hand, we relate the film thickness, in the discussion, to the amount of TiO_2.For both pure TiO_2 and composite films with different thicknesses, there is no shift in Raman E_g peak position (within the error limit). The enhanced Raman peak intensity of different thicknesses of TiO_2 could be interpreted as an increased crystallinity in the TiO_2 film. This could be, in turn, correlated to an enhanced absorption in the UV range and an increased photocatalytic activity of the composite films as well as pure TiO_2 films with different thicknesses on fused silica.

4. Conclusions

We have fabricated and tested composite TiO_2/graphitic-like carbon films with different thicknesses and correlated their optical absorption, structure, and morphology to the observed photocatalytic performance. We have drawn the following conclusions:

(1) Enhanced photocatalytic activity was observed for the composite films in comparison to TiO_2 films with similar thickness.
(2) The enhanced activity was attributed to the synergy effect of carbon at the interface, which aided the separation of photo-generated charge carriers and reduced their recombination probability. This mechanism was also in line with an observed optimum thickness for the enhancement of photo-activity.
(3) The optical measurements showed an enhanced absorption in the visible range for the composite films. The absorption in the UV part also varied with different thicknesses of TiO_2 films. The underlying carbon film caused a red shift of the TiO_2 absorption edge.
(4) Annealing induced a structural change both in carbon and TiO_2, which was confirmed by Raman and XRD. These results also showed that the underlying carbon film reduced the TiO_2 crystallite size in the composite films.

Acknowledgements

The authors would like to acknowledge the financial support by N-INNER through the Solar Hydrogen project (P30938-1 Solväte) and the Foundation for Strategic Environmental Research (Mistra Dnr 2004-118).

References

[1] A. Fujishima, K. Honda, Nature 238 (5358) (1972) 37–38.
[2] S. Ikezawa, et al., Thin Solid Films 386 (2) (2001) 173–176.
[3] B. Oregan, M. Gratzel, Nature 353 (6346) (1991) 737–740.
[4] U. Diebold, Surface Science Reports 48 (5-8) (2003) 53–229.
[5] M. Takahashi, et al., Thin Solid Films 388 (1-2) (2001) 231–236.
[6] R. Asahi, et al., Science 293 (5528) (2001) 269–271.

[7] P. Serp, M. Corrias, P. Kalck, Applied Catalysis A: General 253 (2) (2003) 337–358.
[8] J.H. Park, S. Kim, A.J. Bard, Nano Letters 6 (1) (2006) 24–28.
[9] J.L.F. Philippe Serp, Carbon Material for Catalysis, John Wiley & Sons, Inc., 2009.
[10] L.W. Zhang, H.B. Fu, Y.F. Zhu, Efficient TiO_2 photocatalysts from surface hybridization of TiO_2 particles with graphite-like carbon, Advanced Functional Materials 18 (15) (2008) 2180–2189.
[11] S.U.M. Khan, M. Al-Shahry, W.B. Ingler, Science 297 (5590) (2002) 2243–2245.
[12] Y.J. Chen, J.M. Wu, C.S. Lin, G.Y. Jhan, M.S. Wong, Journal of Vacuum Science & Technology A 27 (4) (2009) 862–866.
[13] A.B. Murphy, Solar Energy Materials and Solar Cells 92 (3) (2008) 363–367.
[14] b. Youji Lia, Xiaodong Lib, Junwen Lic, Jing Yin, Water Research 40 (6) (2006) 1119–1126.
[15] Z.H. Xiaojing Wang, Yujuan Chen, Guohua Zhao, Yafei Liu, Zubiao Wen, Applied Surface Science 255 (7) (2008) 3593–3598.
[16] K. Woan, G. Pyrgiotakis, W. Sigmund, Advanced Materials 21 (21) (2009) 2233–2239.
[17] Y. Yao, et al., Environmental Science & Technology 42 (13) (2008) 4952–4957.
[18] X.Q. Hongtao Yu, Shuo Chen, Huimin Zhao, Journal of Physical Chemistry 35 (111) (2007) 12987–12991.
[19] G. Li, K.A. Gray, Chemical Physics 339 (1-3) (2007) 173–187.
[20] A.G. Sangaraju Shanmugam, S.J. David, C.Y. Jimmy, A. Gedanken, Chemistry of Materials 18 (9) (2006) 2275–2282.
[21] Y.X. Zhibin Lei, Liqin Dang, Wansheng You, Gengshen Hu, Jing Zhang, Chemistry of Materials 19 (3) (2007) 477–484.
[22] A. Modestov, et al., Journal of Physical Chemistry B 101 (23) (1997) 4623–4629.
[23] J.J. Blackstock, et al., Analytical Chemistry 76 (9) (2004) 2544–2552.
[24] J. Besold, et al., Thin Solid Films 293 (1-2) (1997) 96–102.
[25] N.R. Mathews, et al., Solar Energy 83 (9) (2009) 1499–1508.
[26] L.T. Tracy, T. John, J. Yates, Chemical Review 106 (10) (2006) 4428–4453.
[27] Y.-S.W. Po-Wen Chou, Chun-Chu Lin, Yi-Jia Chen, Chia-Liang Cheng, Ming-Show Wong, Surface & Coatings Technology 207 (6–7) (2009) 834–839.
[28] C.G. Gunnar Moos, Roman Fasel, Martin Wolf, Tobias Hertel, Physical Review Letters 87 (26) (2001), 267402-1-4.
[29] N.N. Isao Nakamura, Shuzo Kutsuna, Tatsuhiko Ihara, Shinichi Sugihara, Koji Takeuchi, Journal of Molecular Catalysis A: Chemical 161 (1–2) (2000) 205–212.
[30] W.R. Hosler, R.G. Breckenridge, Physical Review Letters 91 (4) (1953) 793–802.
[31] H. Fredriksson, Applied Physics, Chalmers University, Goteborg, 2009.
[32] J.-Y.L. Jaewon Park, Jun-Hyung Cho, Journal of Applied Physics 100 (11) (2006), 113534 (1–5).
[33] Nalwa, H.S., ed. Handbook of Thin Film Materials Deposition and Processing of Thin Films. vol. 1.
[34] F.I. Toshiaki Ohsaka, Yoshinori Fujiki, Raman spectrum of anatase: TiO_2, Journal of Raman Spectroscopy 7 (6) (1978) 321–324.
[35] R. Loudon, W. Hayes, The Scattering of Light by Crystals, Wiley, Newyork, 1978.
[36] J.C. Parker, R.W. Siegel, Calibration of the raman-spectrum to the oxygen stoichiometry of nanophase TiO_2, Applied Physics Letters 57 (9) (1990) 943–945.
[37] K.R. Zhu, et al., Size and phonon-confinement effects on low-frequency Raman mode of anatase TiO_2 nanocrystal, Physics Letters A 340 (1–4) (2005) 220–227.
[38] Y. Lei, L.D. Zhang, J.C. Fan, Fabrication, characterization and Raman study of TiO_2 nanowire arrays prepared by anodic oxidative hydrolysis of $TiCl_3$, Chemical Physics Letters 338 (4–6) (2001) 231–236.
[39] F.H.P. Sean Kelly, Micha Tomkiewicz, Raman spectroscopy as a morphological probe for TiO_2 Aerogels, Journal of Physical Chemistry 101 (14) (1997) 2730–2734.
[40] K. Paul, L.L. Chu, Characterization of amorphous and nanocrystalline carbon films, Materials Chemistry and Physics 96 (2-3) (2005) 253–277.